# Design and Computational Fluid Dynamics of a Heavy Duty Diesel Engine

**Sena Arıca** ( senaarica@gmail.com )
TOBB ETÜ: TOBB Ekonomi ve Teknoloji Universitesi

**Research Article**

**Keywords:** Computational Fluid Dynamics, Diesel Engines, Combustion, Emission

**Posted Date:** April 26th, 2022

**DOI:** https://doi.org/10.21203/rs.3.rs-1564963/v1

Sena Özlem ARICA, senaarica@gmail.com, Tobb Economy and Technology University, Ankara, TURKEY
Orcid Number: 0000-0003-4620-7878

# DESIGN AND COMPUTATIONAL FLUID DYNAMICS OF A HEAVY DUTY DIESEL ENGINE

**Abstract:** In this study, 1500 hp power class a 12-cylinder Diesel engine, the combustion and emissions are analyzed with the help of Three Dimensional (3D) Computational Fluid Dynamics (CFD). Maximum in-cylinder pressure, temperature, $NO_x$ (Nitrogen Oxides) and soot are obtained. AVL FIRE EseD 3D software is used for the study. Simulation is made for only compression, combustion and expansion strokes when input and output valves are closed. Compression pressure and temperature values are taken as the initial conditions for the simulation from One Dimensional (1D) AVL BOOST program. As there are no measurements available, numerical results are examined for different mesh structures and turbulence models. One eighth of a cylinder, 45 degree sector, is used as the computation domain by making the use of periodic boundary conditions. A mesh study was carried out using a coarse and a 4 times finer mesh. The study revealed that the differences between the coarse and fine mesh results were within the acceptable limits. After that the turbulance model study was done on the coarse mesh. The standard eddy-viscosity based k-ε and non-linear k-ζ-f turbulence models were investigated in terms of $NO_x$ and soot emissions. Finally computations were performed for different combustion models coupled with the k-ζ-f turbulance model.

**Keywords**: Computational Fluid Dynamics, Diesel Engines, Combustion, Emission

### SYMBOLS

| | |
|---|---|
| CFD | Computational Fluid Dynamics |
| CPU | Central Process Unit |
| DKA | Degree Cranck Angle |
| ECFM-3Z | Extended Coherent Flame Model-3 Zone |
| $f$ | Eliptic equation |
| L | Turbulance length scale |
| 1B | One Dimensional |
| 3B | Three Dimensional |
| $S_c$ | Moleculer Schmidt number |
| $S_{c_t}$ | Turbulant Schmidt number |
| ε | Turbulant emit |
| $\nu$ | Kinematic viskozity |
| $\tau$ | Turbulant time scale |
| P | Turbulant kinetic energy production velocity |
| $\nu_t$ | Turbulant kinematic viskosity |

In addition to the design of an engine with right performance characteristics, to comply with internal combustion engine emission standards is also of great importance. Euro emission standards impose a legal obligation for vehicle-producing company. It is not possible to use an engine which doesn't provide European emission standards in a vehicle . For these reasons, ICE, Internal Combustion Engines, the accurate calculation of emissions output is important. In the present study, the most important pollutants Nitrogen Oxides ($NO_x$) and (Soot)

formation and consumption are investigated.

The result of CFD analyses are presented. The pressure and mean temperature curve obtained from 1D analysis are compared with 3D analysis results respectively. BOOST is used for 1D analysis and FIRE is used for 3D analysis. Then; the differences between k-ε and k-ζ-f turbulence models are interpreted.

**Combustion Model- ECFM-3Z**

ECFM-3Z (Extended Coherent Flame Model - Three Zone) is proposed by Colin and Benkenida [1] in 2004. CFM (Coherent Flame Model) and ECFM (Extended Coherent Flame) models are improved for only premixed, spark-ignition (SI) engines but ECFM-3Z model is also used for nonpremixed diffusion flames (Diesel Engine). In this model, in addition to ECFM models, mixture model is added for both single and multiple fuel injections. Each calculation cell is divided into three mixing zones for burnt and unburned gases, so it reveals six different zones for each calculation cells.

Transport equations are solved for average values of $O_2$, $N_2$ ,$CO_2$, CO, $H_2$, $H_2$ O,H,N,OH and NO in ECFM-3Z model. Representative of the transport equation which is solved separately for each chemical species is modeled as follows.

$$\frac{\partial \bar{\rho}\ \tilde{y}_x}{\partial x} + \frac{\partial \bar{\rho}\ \tilde{u}_i\ \tilde{y}_x}{\partial x_i} - \frac{\partial}{\partial x_i}\left(\left(\frac{\mu}{S_c} + \frac{\mu_t}{S_{c_t}}\right)\frac{\partial \tilde{y}}{\partial x_i}\right) = \bar{\dot{w}}_x \qquad (1)$$

$\dot{w}_x$ shows the combustion source term and $\tilde{y}_x$ shows the mass ratio of dissolved chemical components, $S_c$; molecular Schmidt number and $Sc_t$, the turbulent Schmidt number. Fuel is divided into two parts; unburned fuel contained in the gases, $\tilde{y}_{Fu}^u$ and fuel in the burnt gases, $\tilde{y}_{Fu}^b$

$$\tilde{y}_{Fu}^u = \frac{\bar{m}_{Fu}^u}{\bar{m}} = \frac{\bar{m}_{Fu}^u/V}{\bar{m}/V} = \frac{\bar{\rho}_{Fu}^u}{\bar{\rho}} \quad \text{ve} \quad \tilde{y}_{Fu}^b = \frac{\bar{m}_{Fu}^b}{\bar{m}} = \frac{\bar{m}_{Fu}^b/V}{\bar{m}/V} = \frac{\bar{\rho}_{Fu}^b}{\bar{\rho}} \qquad (2)$$

$\tilde{y}_{Fu} = \tilde{y}_{Fu}^u + \tilde{y}_{Fu}^b$ is given in the calculation cell as the average fuel mass. $\bar{m}_{Fu}^u$ is the mass of the fuel in the unburned gas. To calculate $\tilde{y}_{Fu}^u$ the following transport equation is used:

$$\frac{\partial \bar{\rho}\ \tilde{y}_{Fu}^u}{\partial t} + \frac{\partial \bar{\rho}\ \widetilde{u_i}\ \tilde{y}_{Fu}^u}{\partial x_i} - \frac{\partial}{\partial x_i}\left(\left(\frac{\mu}{S_c} + \frac{\mu_t}{S_{ct}}\right)\frac{\partial \tilde{y}_{Fu}^u}{\partial x_i}\right) = \bar{\rho}\tilde{S}_{Fu}^u + \bar{\dot{w}}_{Fu}^u \qquad (3)$$

$\tilde{S}_{Fu}^u$ is the term that shows the amount of evaporation of fuel. $\bar{\dot{w}}_{Fu}^u$ is the source term that takes into account the mix for the unburned and burned region.

**k - $\zeta$ - $f$ Turbulance Model**

In this study, k - ζ - f turbulence model is employed. Turbulent viscosity is given by equation 5 and the transport equations for ζ is given by equation 8.

$$P = \mu_t \left(\frac{\partial \tilde{u}_i}{\partial x_j} + \frac{\partial \tilde{u}_j}{\partial x_i}\right)\frac{\partial \tilde{u}_i}{\partial x_j} \quad (4)$$

Turbulent viscosity $\nu_t$ is given by equation 5.

$$\nu_t^{\zeta} = C_{\mu}\zeta k\tau \quad (5)$$

$$\frac{Dk}{Dt} = P - \varepsilon + \frac{\partial}{\partial x_j}\left[\left(\nu + \frac{\nu_t}{\sigma_k}\right)\frac{\partial k}{\partial x_j}\right] \quad (6)$$

Ɛ in Equation 6 shows turbulent diffusion, k; turbulent kinetic energy, ν; kinematic viscosity, τ ; turbulent time scale, P shows the production rate of turbulent kinetic energy.

$$\frac{D\varepsilon}{Dt} = \frac{C_{\varepsilon 1}P - C_{\varepsilon 2}\varepsilon}{\tau} + \frac{\partial}{\partial x_j}\left[\left(\nu + \frac{\nu_t}{\sigma_\varepsilon}\right)\frac{\partial \varepsilon}{\partial x_j}\right] \quad (7)$$

$$\frac{D\zeta}{Dt} = f - \frac{\zeta}{k}P + \frac{\partial}{\partial x_k}\left[\left(\nu + \frac{\nu_t}{\sigma_\zeta}\right)\frac{\partial \zeta}{\partial x_k}\right] \quad (8)$$

$$L^2\nabla^2 f - f = \frac{1}{\tau}\left(c_1 + C_2'\frac{P_k}{\varepsilon}\right)\left(\zeta - \frac{2}{3}\right) \quad (9)$$

$$\tau = max\left[\min\left(\frac{k}{\varepsilon}, \frac{0.6}{\sqrt{6}C_\mu|S|\zeta}\right), C_\tau\left(\frac{\nu}{\varepsilon}\right)^{1/2}\right] \quad (10)$$

$$L = C_L\, max\left[\min\left(\frac{k^{3/2}}{\varepsilon}, \frac{k^{1/2}}{\sqrt{6}C_\mu|S|\zeta}\right), C_\eta\left(\frac{\nu^3}{\varepsilon}\right)^{1/4}\right] \quad (11)$$

The following values for the coefficients used in the equations are taken. Cμ = 0.22, $\sigma_\zeta = 1.2$ $c_1 = 0.4$ , $C_2' = 0.65$, $C_\tau = 6$, $C_L = 0.36$ and $C_\eta = 85$.

## Results

Comparison of One-Dimensional and Three-Dimensional Results

In Figure 1, it is seen that in cylinder pressure is the same both 1D and 3D analysis up to 702 DCA which combustion starts. After the start of burning, since the fuel burns faster, while the maximum pressure is reached at 725 DCA with 154 bar in 3D analysis, it is 143 bar at 732 DCA in 1D gas exchange analysis. Its reason is about the longer ignition delay at 1D analysis. After the finish of injection, at 738 DCA, the pressure which is calculated at 1D analysis is 20 bar higher than 3D analysis. Because the piston bowl geometry is not known and while ECFM-3Z combustion model is used on 3D analysis, AVL MCC model is used on 1D analysis.

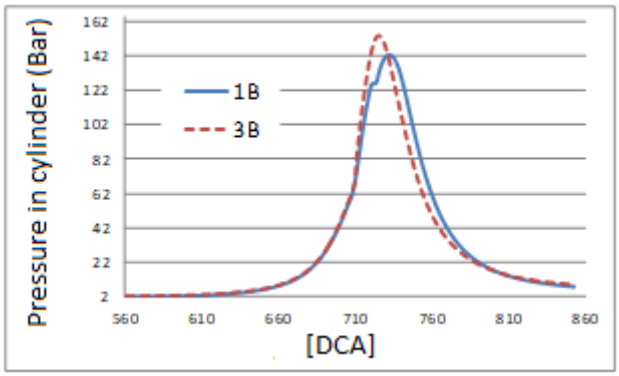


**Figure 1.** The change of in cylinder pressure according to cranck angle on 1D (one-dimensional) and 3D (three dimensional) calculations

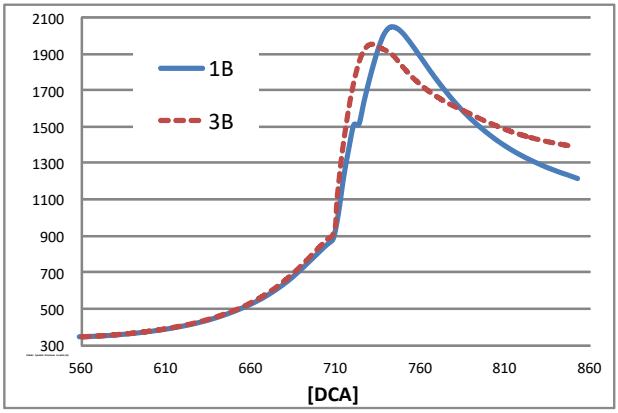


**Figure 2.** The change of in cylinder temperature according to cranck angle on 1D (one-dimensional) and 3D (three dimensional) calculations

The average temperature inside the cylinder according to crank angle for 1D and 3D analyses is shown in Figure 2 . When analyzing this chart, it is seen that temperature curve follows pressure curve in Figure 1. Since the fuel burns faster at the start of combustion at 3D analysis, in cylinder temperature is higher at 3D analysis than 1D analysis at the start of combustion. However, towards the end of combustion, it is observed that while maximum temperature reaches about 2050 K at 1D analysis, it is around 1950 K at 3D analysis.

## Numerical Study on Mesh Size

To see the effect of cell number, two mesh sizes are used with 55 000 and 200 000. Temperature, velocity, equivalence ratio, $NO_x$ and soot mass rate changes are compared along the injection line. Injection line length which is shown in Figure 3 is about 4 cm.

**Table 1.** Mesh Size and Related Properties

| Numerical Mesh Size | CPU |
|---|---|
| 55.000 | 1 day |
| 200.000 | 7 days |

While the results can be obtained in 1 day with 55.000 cells, it takes almost 7 days with 200.000 cells. Solutions are obtained with 64-bit operating system on a personal computer using a single CPU.

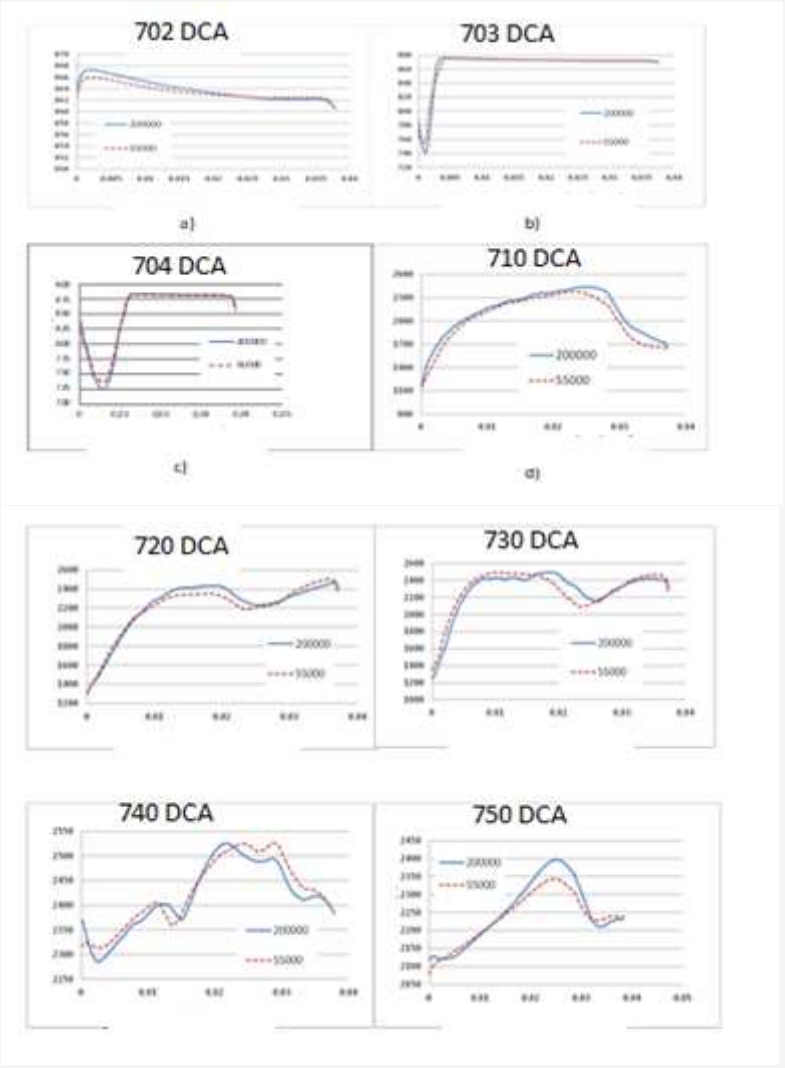


**Figure 3.** The change of temperature according to mesh size along the injection arc length for 702, 703, 704, 710, 720, 730, 740, 750 DCA

As it is seen from Figure 3 , early in the 702, 703 and 704 DCA , temperature values both thin and coarse mesh structure are very close together. The difference is about %1-2 at 702, 703 and 704 DCA, % 4-5 at 710 and 720 DCA , about 8% at 730 DCA , 2-3% at 740 and 750 DCA.

At the start of spraying, at 702 DCA, the temperature in the cylinder is around 865K. After spraying the fuel at 350K and the evaporation, the temperature decreases to 770 K at 703 DCA. Since the injection temperature of the fuel is much lower than the cylinder temperature, the temperature in the cylinder decreases suddenly. Maximum temperature, 2520 K is reached at 740 DCA near the end of the combustion.

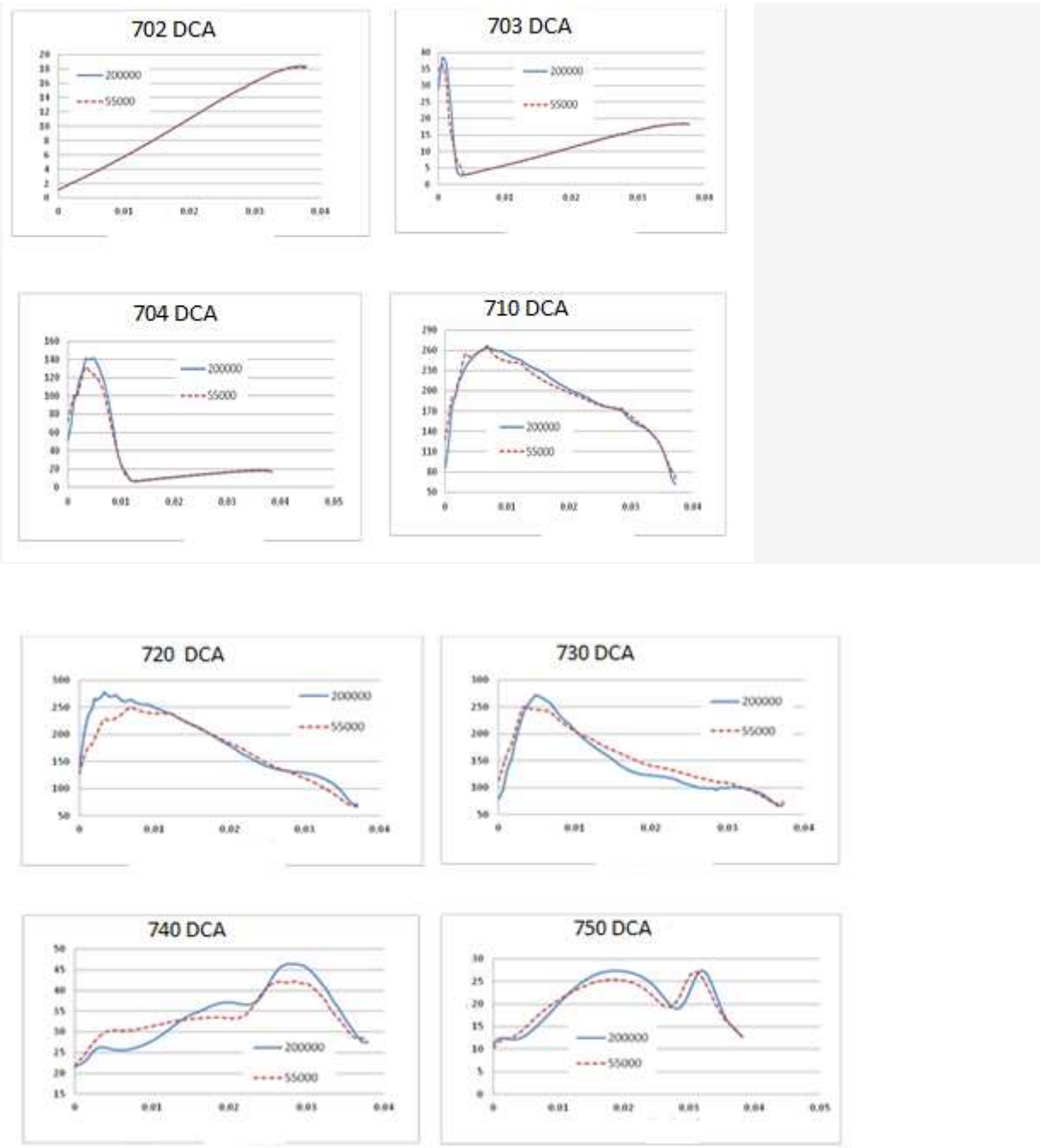


**Figure 4.** The velocity along the injection line : 702,703, 704, 710, 720, 730, 740, 750 DCA

While the velocity along the injection line decreases from the first 1 cm part of injection line at the start of the injection, it can not be seen many differences between the first 1 cm and 4 cm portions of the injection line since the fuel evaporates completely towards the end of the combustion.

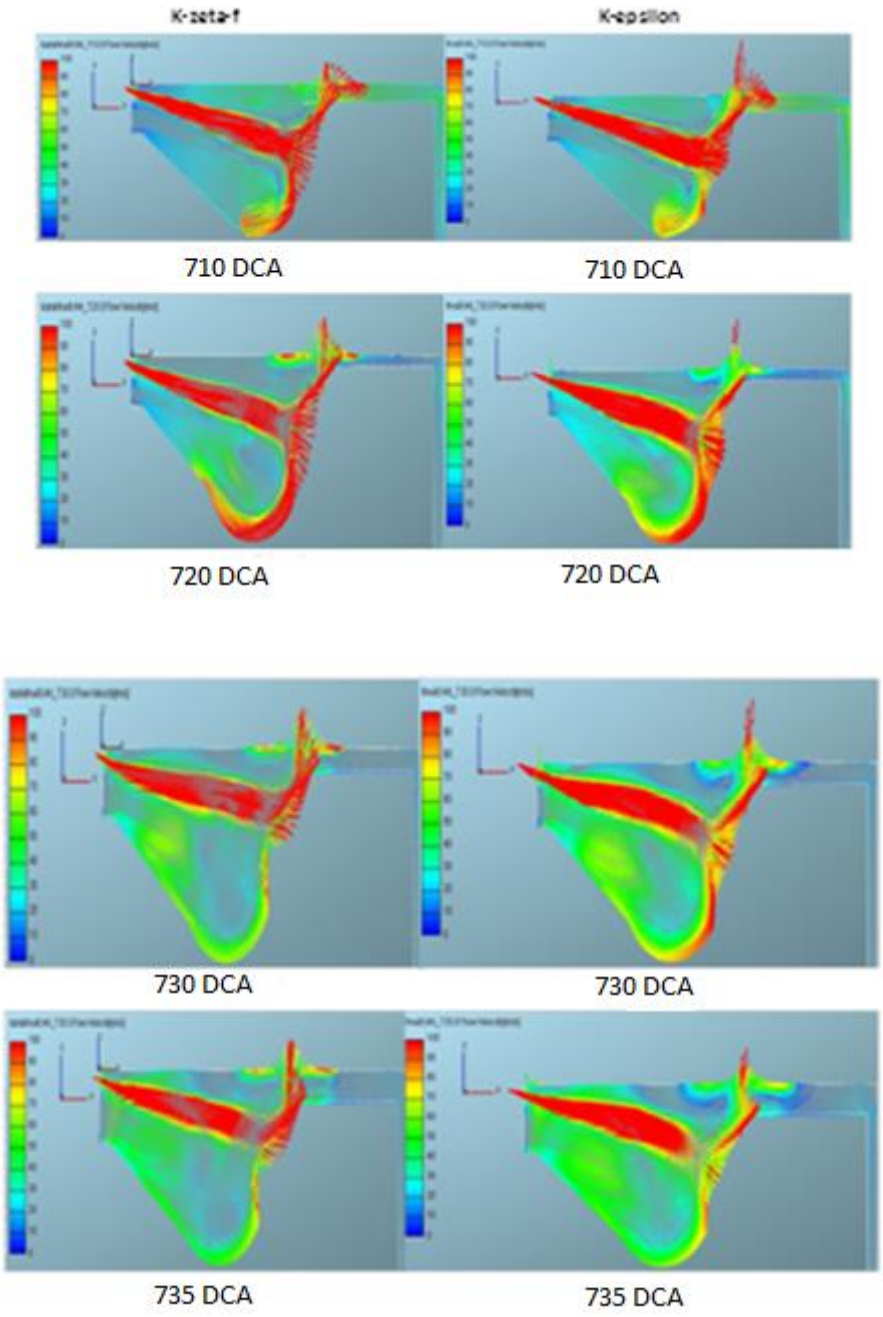


**Figure 5.** Velocity vectors for k-ζ-f and k-ε turbulence models between 710-735 DCA

The squish motion which is a general engine movement can be seen in Figure 5. Squish is the movement of the gases to the center which is trapped between the piston surface and the cylinder head while the piston is going up. If this movement is in the piston bowl, it creates a vertical motion (tumble). The flow hits the wall and returns back, this leads to the formation of the vortex is called squish. Although the difference of the turbulence models affect velocity vectors numerically, it doesn't affect much directionally.

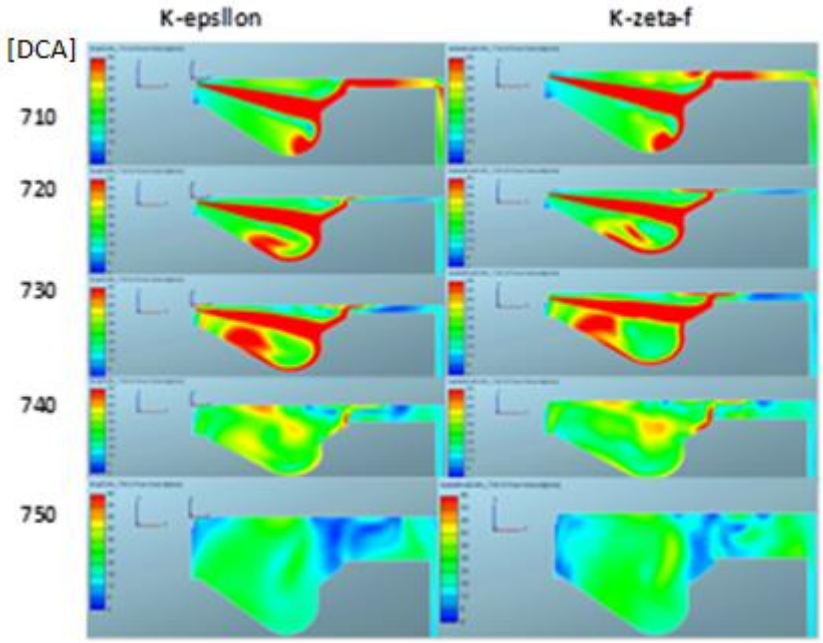


**Figure 6**. Velocity contours for different turbulence models between 710-750 DCA

The scale in velocity contours in Figure 6 is between 0-60 m/s. As it is seen from the contours, the velocity doesn't differ too much for different turbulance models. Velocity is about 20 m/s higher at k-ζ-f turbulance model at piston walls.

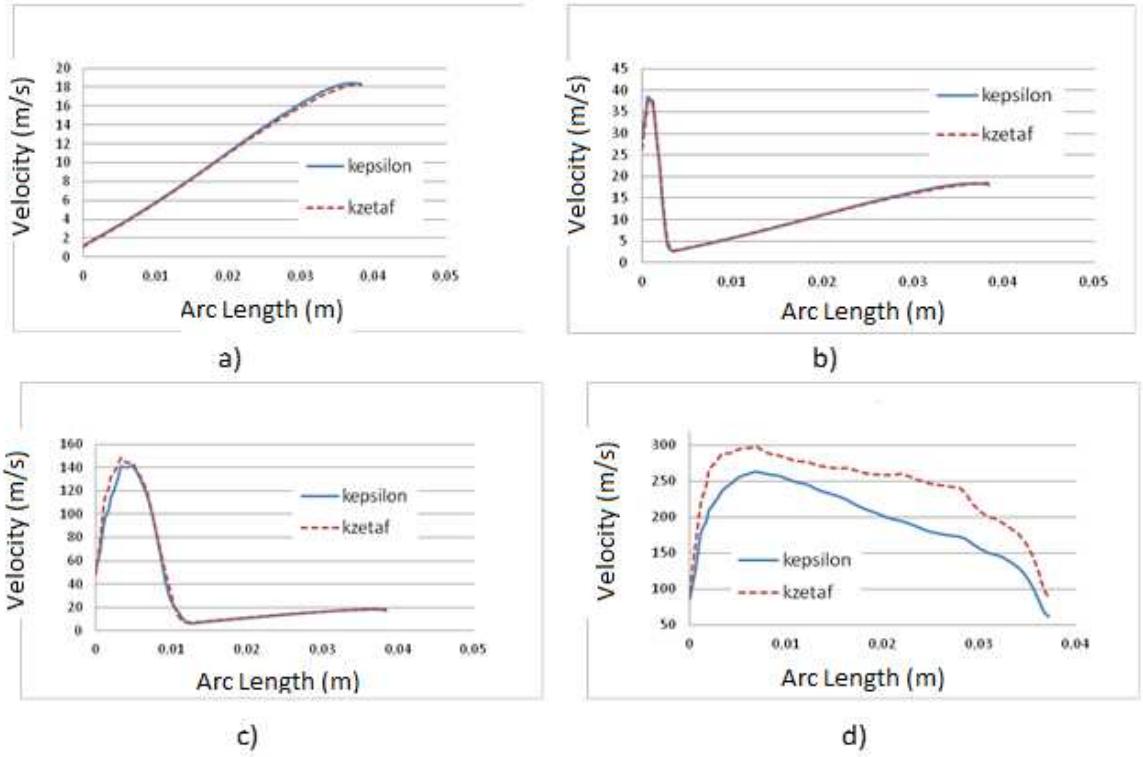


**Figure 7.** The velocity along the injection line for different turbulence models

At the beginning of the combustion, if the velocity along the injection line is considered in Figure 7, there is not seen any significant differences between k-ε and k-ζ-f turbulance

models. It is seen that the velocity values in k-ζ-f turbulance model are about %40 higher than k-ε turbulance model through the end of combustion. It says that k-ζ-f turbulance model may have provided a better mixture.

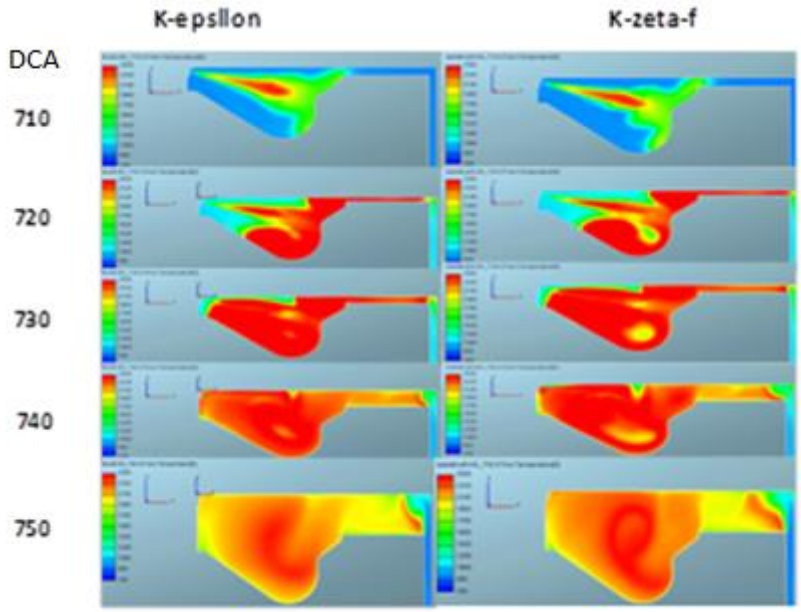


**Figure 8.** Temperature contours for different turbulance models for 710-750 DCA

The temperature contours are seen which follow the middle of the section in the piston for the interval of 700-2500 K for k-ε and k-ζ-f turbulance models in Figure 8. As it is seen from the figure, the temperature is calculated about 100 K higher than k-ε turbulance model.

**Table 2.** Average Nitrogen Oxide (NO) in the exhaust and mean unburned fuel (UHC) emissions

| | NO [ppm] | Unburned Fuel [ppm] |
|---|---|---|
| **k-ε** | 284 | 1140 |
| **k-ζ-f** | 476 | 737 |

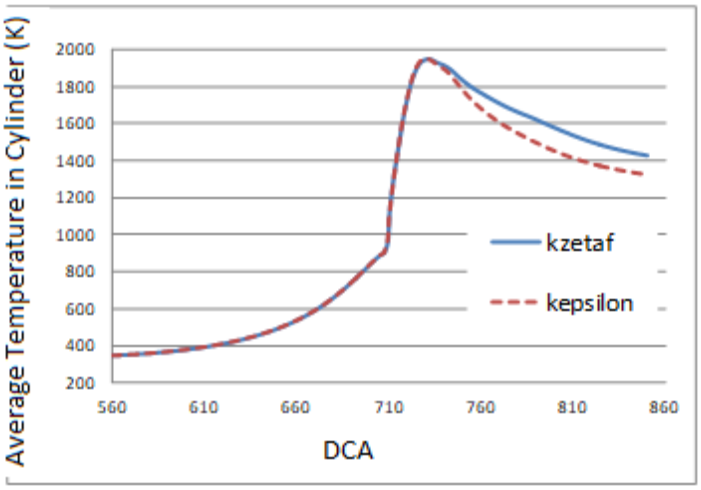


**Figure 9.** The average temperature values for different turbulence models in cylinder

Average temperature in cylinder is observed for k-ζ-f and k-ε turbulence models in Figure 9. As it is seen from the figure although there is not seen any significant differences at average temperature values, through the end of combustion from about 740 DCA, it is seen that k-ζ-f turbulance model calculates the average temperature about 100 K higher. Its reason can be understood from unburnt fuel quantity and the velocity contours in Table 2. Unburned fuel quantity is 400 ppm higher than k-ζ-*f* turbulance model in k-ε turbulence model so that it can be thought that k-ζ-*f* turbulance model creates a better mixture. At the same time it is known that k-ζ-*f* turbulance model calculates the temperature more precisely near of the walls. It explains why temperature is higher than k-ε turbulence model in k-ζ-*f* turbulance model.

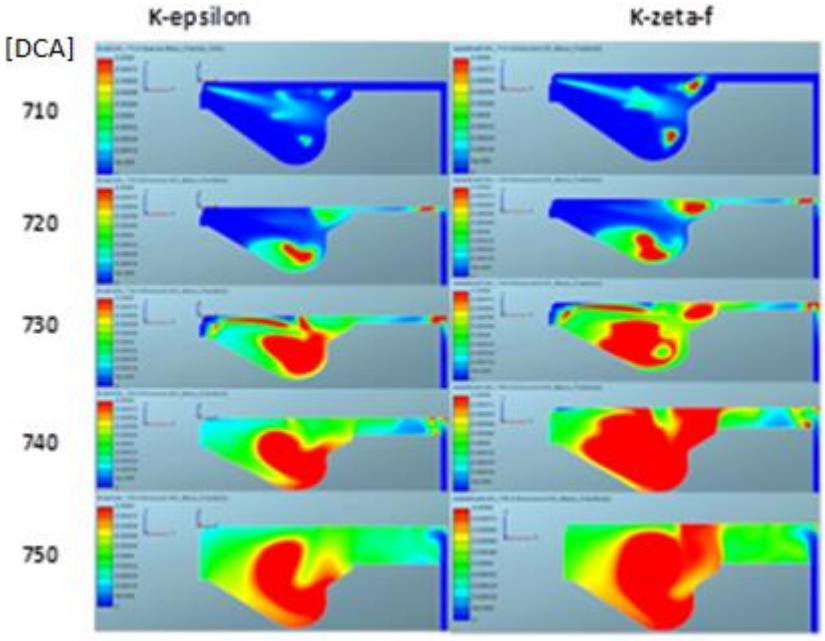


**Figure 10.** NO mass ratio contours for different turbulance models between 710-750 DCA

It is seen that temperature graphs follow NO mass ratio graphs. Since the temperature values are higher in k-ζ-f turbulence model, it affects thermal NO mass ratio values and causes high thermal NO mass ratio values.

As it is seen from Table 2, in k-ε turbulance model, since the amount of unburned fuel is more than k-ζ-f turbulance model, temperature values and NO emissions are lower in k-ε turbulence model.

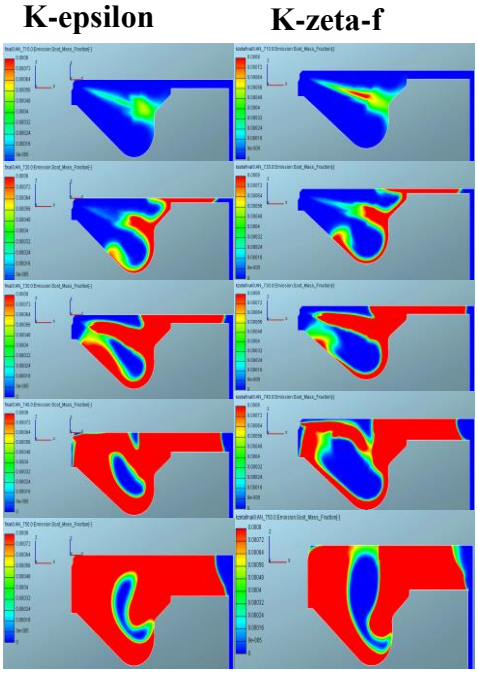


**Figure 11.** Soot mass ratio contours along the injection line for different turbulance models between 710-750 DCA

The soot mass ratio contours are seen which follow the middle of the section in the piston for the interval of 0-0.0008. When the contours are analyzed, at the start of the combustion, soot mass ratio is higher in k-ζ-f turbulence model between 710-720 DCA but after 720 DCA it is higher in k-ε turbulence model. Since the temperature is higher in k-ζ-f turbulence model, soot is burned better and less than k-ε turbulence model.

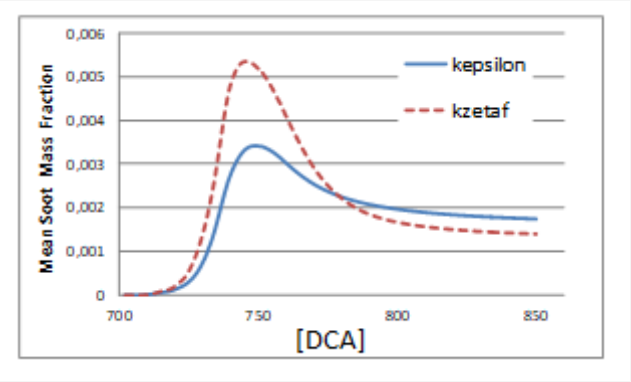


**Figure 12.** The change of mean soot mass fractions according to DCA for different turbulance models

When the figure 12 is analyzed, it is seen that mean soot mass ratio is higher from the start of combustion to the end of it in k-ζ-f turbulence model but after the end of combustion, these values are less than k-ε turbulence model. It is supported by the soot mass ratio contours in Figure 11. The soot in cylinder is burned better in k-ζ-f turbulence model. Since the temperature is higher than k-ε turbulence model at 750 DCA, mean soot mass ratio is also higher in k-ζ-f turbulence model.

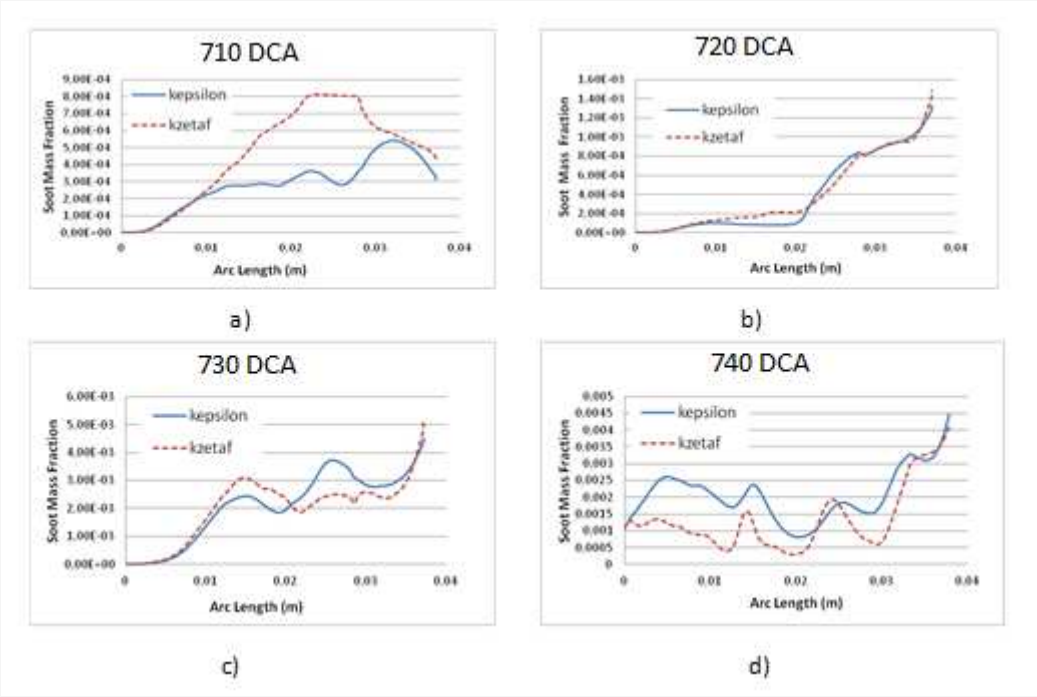


**Figure 13.** Soot mass ratio along the injection line for different turbulence models

It is seen that Figure 11 supports Figure 13. Akihama and his co-workers [2] show that soot is seen when the temperature is between 1500 K and 2400 K and the equivalence ratio is higher than 2. Andersson and his co workers [3] observe that soot is burned at low equivalence ratio. It can be said that soot occurs between approximately 704-730 DCA and it starts to burn after 730 DCA.

## RESOURCES


[1] Colin, O ve Benkenida , The 3-Zones Extended Coherent Flame Model (ECFM3Z) for Computing Premixed/Diffusion Combustion, Oil and Gas Science and Technology,2004043,2004

[2] Akihama, K., Takatori, Y., Inagaki, K., Sasaki, S., ve Dean, A., Mechanism of the smokeless rich Diesel combustion by reducing temperature, SAE, 2001-01-0655, 2001.

[3] Andersson, O., Somhorts, J., Lindgren, R., Blom, R., ve Ljungqvist, M., Development of the Euro 5 Combustion System for Volvo Cars' 2.4 l Diesel Engine, SAE, 2009-01-1450, 2009.

[4]Arıca, S., Ö., Ağır Vasıta Bir Dizel Motorun Tasarımı, Üç Boyutlu Hesaplamalı Akışkanlar Dinamiği ve Emisyon Analizi, Yüksek Lisans Tezi, Tobb Ekonomi ve Teknoloji Üniversitesi, Fen Bilimleri Enstitüsü, Ankara, 2012.

[5]Fridriksson, H., S., 2011, On CFD Analysis of Heat Transfer of a Heavy Duty Diesel Engine, *Yüksek Lisans Tezi, Lund Üniversitesi*, İsveç.

[6] AVL FIRE v2011 user manual, 2011